J.Serb.Chem.Soc. 67(4)291–300(2002)
JSCS-2950

UDC 548.2:546.657:666.293.35
Original scientific paper

The growth of Nd: YAG single crystals

ALEKSANDAR GOLUBOVIĆ[1*#], SLOBODANKA NIKOLIĆ[1], RADOŠ GAJIĆ[1], STEVAN ĐURIĆ[2] and ANDREJA VALČIĆ[3]

[1]Institute of Physics, Pregrevica 118, P. O. Box 57, YU-11001 Belgrade, [2]Faculty of Mining and Geology, Đušina 7, P. O. Box 162, YU-11000 Belgrade and [3]Faculty of Technology and Metallurgy, Karnegijeva 4, YU-11000 Belgrade, Yugoslavia

(Received 17 October, revised 17 December 2001)

$Y_3Al_5O_{12}$ doped with 0.8 % wt. Nd (Nd:YAG) single crystals were grown by the Czochralski technique under an argon atmosphere. The conditions for growing the Nd: YAG single crystals were calculated by using a combination of Reynolds and Grashof numbers. The critical crystal diameter and the critical rate of rotation were calculated from the hydrodynamics of the melt. The crystal diameter D_c = 1.5 cm remained constant during the crystal growth, while the critical rate of rotation changed from ω_c = 38 rpm after necking to ω_c = 13 rpm at the end of the crystal. The value of the rate of crystal growth was experimentally found to be 0.8–1.0 mm/h. According to our previous experiments, it was confirmed that 20 min exposure to conc. H_3PO_4 at 603 K was suitable for chemical polishing. Also, one-hour exposure to conc. H_3PO_4 at 493 K was found to be suitable for etching. The lattice parameter a = 1.201 (1) nm was determined by X-ray powder diffraction. The obtained results are discussed and compared with published data.

Keywords: Czochralski technique, Nd:YAG, growth, single crystal, etching.

INTRODUCTION

Oxide crystals are of great importance for modern electrical and electro-optical applications in several devices. Diode-pumped Q-switched solid-state lasers have been demonstrated to have high-efficiency, high average power, and high energy per pulse. The applications of Q-switched lasers are well known: lidars, remote sensing, pollution detection, nonlinear optical processes, and material processing.[1,2]

Nonlinear optical conversion techniques, like second-harmonic generation (SHG or frequency doubling) or like optical parametric oscillation (OPO) can be used not only to extend the frequency range of existing lasers, but also to allow the set up of non-destructive testing methods to determine the properties of materials of interest for

* Corresponding author, E-mail: galek@EUnet.yu.

Serbian Chemical Society active member.

integrated optical applications. In principle, any crystalline medium without inversion symmetry can produce SHG, provided the electric field *E* of the electromagnetic radiation is sufficiently large, as for instance in the high peak power of pulsed laser systems lika a Q-switched Nd:YAG laser.[3] Recently, the possibility of multiple applications of lasers in dentistry, beyond soft tissue surgery and dental compositeuring, were found.[4] These include replacement of the dental drill with a laser, laser dental decay prevention, and laser decay detection, but, unfortunately, they have not yet been realized clinically.

There has been a continuing interest in the development of the technology of $Y_3Al_5O_{12}$ (YAG) garnet crystal growth because Nd-doped YAG is one of the most important laser hosts for the generation of 1.06 μm infrared radiation. Its good optical, chemical and mechanical characteristics have made it the standard material in industrial applications were reliability is particularly important. Nd:YAG crystals are usually grown by the conventional Czochralski (CZ) technique.[5–8] Besides that, for miniature laser sources Nd:YAG can grow by the micropulling-down (μ-PD) technique[9–11] and by the crucibles laser heating pedestal method.[12–14]

The shape of melt/crystal interface is strongly affected by internal radiant heat transfer through the crystal and this mechanism promotes deeply deflected interfaces toward the melt.[15] The deep interfaces in these systems can lead to detrimental features in the grown crystal, notably the production of highly strained regions near the core of the crystal, which correspond to facet formation along the melt/crystal interface during growth.[16,17] The appearance of a core is typical for $Bi_{12}SiO_{20}$, $Bi_{12}GeO_{20}$ and Nd:YAG crystals. Applying both theoretical and experimental investigations, we successfully obtained $Bi_{12}SiO_{20}$[18] and $Bi_{12}GeO_{20}$[19] single crystals. In our previous experiments,[20–22] we obtained Nd:YAG single crystals with a core, despite taking some hydrodynamics equations into account. The aim of our work was, by applying both theoretical and experimental treatment, to produce and characterize Nd:YAG single crystals without a core.

EXPERIMENTAL

Yttrium aluminium garnet doped neodymium single crystals (Nd:YAG) were grown by the Czochralski technique using a MSR 2 crystal puller, as described previously.[23] The atmosphere used was argon. The starting materials were powdered Y_2O_3, Al_2O_3 and Nd_2O_3 (all Koch&Light) all of 4N purity. Powdered ZrO_2 (Koch&Light) of 4N purity was used for isolation. The purity of argon (Tehnogas) was 4N. The iridium crucible (4 cm diameter, 4 cm high) was placed into an alumina vessel surrounded by ZrO_2 wool isolation. Double walls were used to protect the high radiation. To decrease the radial temperature gradient in the melt, alumina was mounted around all the system. The pull rates were generally in the range 0.8–3 mm/h, and the best results were obtained with a pull rate of 1 mm/h. The crystal rotation rates were between 6 and 100 rpm. The best results were obtained with a crystal rotation of 20 rpm. The diameters of crystals were between 10 and 20 mm. The crucible was not rotated during the growth. After the growth run, the crystal boule was cooled at a rate of about 50 K/h down to room temperature.

Various solutions of H_3PO_4 at different temperatures and for various exposure times were tried for chemical polishing and etching. For chemical polishing, exposure to a concentrated (85 %) solution of H_3PO_4 at 603 K for 20 min was confirmed to be suitable, as was found in our previous work.[20–21] Exposure for one hour to an 85 % solution of H_3PO_4 at 493 K after was found to be a suitable for etching.[21–22]

All the obtained crystal plates were observed in polarized light to visualize the presence of a core and/or striations.

The chemical compositions of the products were determined by powder XRD analysis. All the samples were examined under the same conditions, using a Philips PW 1729 X-ray generator, a Philips 1710 diffractometer and the original APD software. The radiation source was an X-ray LLF tube with copper radiation and a graphite monochromator. The radiation was $\lambda CuK\alpha_1 = 0.15460$ nm. The anode tube load was 40 kV and 30 mA. Slits of 1.0 and 0.1 mm were fixed. The samples were pressed into standard aluminium frames and measured in the 2θ ranges from 5º to 60º. Each 1/50º (0.02º) was measured for 0.5 s. For production identification, the MPDS program and JCPDS (ASTM) card files were used.

RESULTS AND DISCUSSION

The growth of crystal from the melt is one of the most important techniques for producing advanced materials. A successful growth requires the control of heat and mass transfer in the melt and through the phase boundaries. In the case of the Czochralski technique (CZ), different types of convection are generated in the melt: natural convection due to density differences in the gravity field and to thermocapillary forces at the melt-gas interface, and forced convection caused by the rotation of the crystal and/or the crucible.[24] These different flows influence the shape of the melt/crystal interface during growth, which in turn affects the quality of the grown crystal. It has been experimentally established that the flatter this interface is, the better the quality of the grown crystal.[25] The objective is always to find the experimental growth conditions which produce a planar interface during the entire pulling process.

In our previous experiments[20–22] we tried to obtain a planar interface during the growth of a Nd:YAG crystal by applying the equations taken from Takagi[26] and Carruthers.[27] It is well known that a crystal/melt interface becomes flat at the moment of the inversion in the shape of the crystal/melt interface. This phenomenon results from changes in the movements of the melt. Simultaneously, a certain part of the crystal is melting thus causing the crystal/melt interface, convex till then, to become almost flat *versus* the melt. At the moment of inversion, the diameter of the crystal reaches its critical value for a particular rotation (a critical rotation). Using Takagi equation,[26] one obtains a plot of D_c (the critical diameter) *versus* $\omega_c^{-1/2}$ (the critical rate of rotation), where almost all points belong to the line. The value of ω_c was 70 rpm, D_c was 15 mm, and the pulling rate was experimentally found to be 1.2–1.3 mm/h. However, all crystals had a core although inversion occurred.

Using equations derived from Carruthers ($Gr=Re^2$ assuming that the melt density does not change during the process of crystal growth), one obtains D_c = 10 mm, ω_c = 100 rpm, with an experimentally determined pulling rate of 3 mm/h. All these crystals also had a core of about 1.5 mm in diameter.

Xiao and Derby[28] were the first to calculate deeply convex interfaces during CZ oxide growth and showed that such shapes were caused by internal radiation through the crystal coupled with convective heat transfer in the melt. It is well known that the Prandtl number serves as a measure of the relative importance of the transfer of heat by conduction and by convection. The Prandtl number ($Pr = \nu/\alpha$) is a material property,

and typical values are 0.01 for molten metals and semiconductors, and 1 for molten oxides. It was found[29] that for YAG crystals the thermal conductivity (k) and thermal expansion coefficient (α) strongly depend on the temperature. The thermal conductivity can be calculated using the following equation:

$$kT = \frac{a}{[(\ln(bT)]^c} - \frac{d}{T} \tag{1}$$

where $a = 1.9\times10^6$ W/cm K, $b = 5.33$ K^{-1}, $c = 7.14$, and $d = 331$ W/cm and a by the relation:

$$\alpha(T) = aT^b \tag{2}$$

where $a = 1.14\times10^{-7}$ K$^{-(b+1)}$ and $b = 0.69$.

Our results can be discussed in terms of the rotational Reynolds number (Re) and the Grashof number (Gr), which are defined as:

$$Re = \rho\, R_{crys.}^2\, \omega_s/\mu \tag{3}$$

$$Gr = \rho^2\, g\, \beta\, \Delta T\, R_{cruc.}^3/\mu^2 \tag{4}$$

Where ρ is the melt density, $R_{crys.}$ is the crystal radius, ω is crystal rotation rate, μ is the viscosity of the melt, g is the acceleration of the free fall, and β is the thermal expansion coefficient, ΔT is the difference between the maximum melt temperature (which occurs along the inner crucible wall) and the melting point temperature, and $R_{cruc.}$ is the inner radius of the crucible. These dimensionless numbers represent measures of the driving forces for flows induced by crystal rotation (Re) and buoyancy (Gr). The thermophysical properties employed for our calculation, which represent the most recent physical property measurements of YAG,[30] are shown in Table I.

The Marangoni number (Ma) is a measure of surface tension driven flows and given by[31]:

$$Ma = -(\partial\gamma/\partial T)\, \Delta T\, (R_{cruc} - R_{crys.})\, (\rho\, \nu\, \alpha)^{-1} \tag{5}$$

where $(\partial\gamma/\partial T)$ is the temperature coefficient of the surface tension; ΔT the temperature difference ($T_{crucible} - T_{mp}$); $R_{crus.}$ the crucible radius; $R_{crys.}$ the crystal radius; ρ the melt density; ν the kinematic viscosity, and α the thermal diffusivity of the melt. For YAG crystals, $(\partial\gamma/\partial T) = 0$ and the Marangoni number cannot be used.

The thermal zone is heated by the Joule effect. In this configuration, the temperature is larger at the bottom of the crucible than at the height of the melt/crystal interface. The resulting conditions at the walls of the crucible ($T_{cruc.}$) and of the crystal ($T_{crys.}$) are about 2281 to 2251 K and 2243 K, respectively, as the temperature of the crucible, $T_{cruc.}$ ($R_{cruc.}$, z), decreases during the process and the temperature difference, ΔT, between the

crucible and the crystal at the free surface is not exact. From the temperature data at the walls of the furnace and the crucible, it was estimated[25] that this difference varies according to $\Delta T = 8\,h \pm 0.5$ (here h is the height of the melt in cm and T is degrees in Celsius). Applying the Carruthers[27] relation $Gr = Re^2$, crystal necking values for a critical diameter $D_c = 1.5$ cm and a critical rotation rate $\omega_c = 28$ rpm were found. At the bottom of the crystal, ω_c was calculated to be 13 rpm. The rotation rate of the crystal was programmed to decrease linearly with the melt height from about 28 rpm at the start to about 13 rpm at the end of the pulling. The pulling rate was experimentally found to be 0.8–1.0 mm/h. The growth parameters are given in Table II.

TABLE I. Thermophysical properties of YAG crystals where the subscripts m, crys, cruc. and i denote melt, crystal, crucible, and insulation, respectively

Discriptionm, unit	Symbol	Value
Density/[g/cm^3]	φ_m	3.6
Density/[g/cm^3]	$\varphi_{crys.}$	4.3
Density/[g/cm^3]	$\varphi_{cruc.}$	22.4
Density/[g/cm^3]	φ_i	5.6
Emissivity	ε_m	0.3
Emissivity	$\varepsilon_{crys.}$	0.3
Emissivity	$\varepsilon_{cruc.}$	0.5
Emissivity	ε_i	0.8
Heat capacity/[J/g K]	c_{pm}	0.8
Heat capacity/[J/g K]	$c_{pcrys.}$	0.8
Heat capacity/[J/g K]	$c_{pcruc.}$	1
Heat capacity/[J/g K]	c_{pi}	1
Heat of fusion/[J/g]	ΔH_f	455.4
Melting point/[K]	T_f	2243
Surface tension/[dyn/cm]	γ	781
Thermal conductivity/[W/cm K]	k_m	0.04
Thermal conductivity/[W/cm K]	$k_{crys.}$	0.08
Thermal conductivity/[W/cm K]	$k_{cruc.}$	1.5
Thermal conductivity/[W/cm K]	k_i	0.03
Melt expansivity/[K^{-1}]	β	1.8×10^{-5}
Thermocapillary coefficient/[dyn/cm K]	$d\gamma/dT$	0
Viscosity/[g/cm s]	μ	0.46

The low-gradient Nd:YAG simulations presented here exhibited a smoothly convex interface associated with successful flat-interface growth. The high-gradient Nd:YAG simulations yielded complicated, wavy melt/crystal interfaces, which resisted inversion at higher rotation rates. Our calculations also established that the nature of the inversion transition is strongly affected by the process conditions where the transition

can occur over a wide range of rotation rates and can exhibit hysteresis or smooth transitions between states.[15] In fact, the results presented here offer compelling arguments against the general usefulness of simple scalings[27,32] or universal correlations[33–35] to describe the mechanism of interface inversion during Czochralski growth of oxide crystals.

TABLE II. Experimental conditions for the growth of Nd:YAG crystals

Parameter	Value
Crystal radius/cm	1.5
Crucible radius/cm	4
Crucible height/cm	4
Average temperature of zone during growth/K	2262
Average crystal pulling rate/mm/h	0.9
Average crystal rotation rate/rpm	20

The interaction on the geometry of the growing crystal of the exterior thermal environment *via* radiant heat transfer is a well-known factor in Czochralski growth processes. Internal radiant heat transfer magnifies the importance of these interactions with respect to the formation of a temperature field within the crystal. A large cone angle results in significant temperature gradients near the corner of the shoulder region, which could promote crystal cracking due to the greater, associated thermal stresses. This effect has been observed in an experimental system,[36] and has lead to the adoption of rather small cone angles in common practice. It was found[15] that a cone angle of 35º represents a common choice for YAG growth and produces relatively small radial temperature gradients through the crystal, while growth with a larger cone angle, such as 75º, forces the crystal shoulder to point more directly upwards, towards the coolest portion of the growth enclosure. This change in the crystal geometry increases the overall heat loss through the crystal, resulting in a more deeply deflected melt/crystal interface.

Fig. 1. A view of an obtained Nd:YAG single crystals plate. It can be seen to be withont a core.

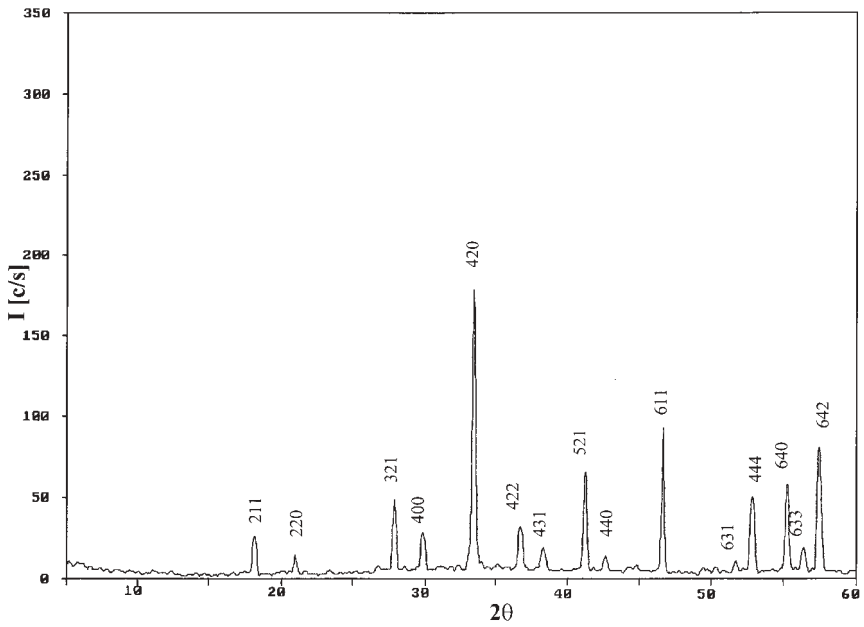

Fig. 2. X-Ray pattern of a powdered Nd:YAG single crystal.

We observed[21] some formed facets on those parts of the melt/crystal interface that were parallel to the facets [211] and [110]. There was a core into these crystals although an attempt was made to grow the crystal according to the results obtained after application of hydrodynamics in the melt equations. According to newer results from the literature,[15] the main reason for the appearance of a core is a large cone angle during necking. We used a cone angle of ~ 30º for Nd:YAG single crystal growth and obtained crystals without a core. A picture of an obtained Nd:YAG single crystal plate is shown in Fig. 1.

Flat-interface growth of YAG is difficult to achieve, especially for neodymium-doped material. However, it was reported[15,37] that flat-interface Nd:YAG single crystals growth can be achieved by applying a low thermal gradient. Xu *et al.*[37] employed a massive baffle over the melt to promote extreme thermal gradients, while Xiao *et al.*[15] used a two-zone furnace. For this purpose, we used an alumina tube in our crystal growth experiments.

The structural properties were obtained using X-ray diffraction analysis of powdered samples. A Philips PW 1710 diffractometer was used in the 2θ ranges from 5º to 60º. The unit cell of Nd:YAG was calculated by the least square method using 15 reflections including more $K\alpha_2$ for 1 reflection. All the reflections correspond to Nd:$Y_3Al_5O_{12}$ crystals and gave the parameter of the cubic unit cell a = 1.2103 (2) nm.[38] Some divergence from the compared results can be explained by the fact that X-ray powder diffraction analysis gives a statistical result. Our calculated result for the lattice parameter is a = 1.201 (1) nm, which is in good agreement with published data.[1,5,7] An X-ray difractogram for powdered Nd:YAG is given in Fig. 2.

The intensities of the reflections for some crystal planes, together with their Mueller indices and distances between the reflection planes are given in Table III. The intensities of the reflections from Fig. 2 are given together with published intensities for the same planes in JCPDS ("Joint Committee on Powder Diffraction Standards"). Some divergences between the experimentally obtained 2θ values and the literature ones could be explained as being a consequence of the used wavelength CuKα1 (0.15406 nm) and CuKα1 cited in the literature[38] (0.15418 nm).

TABLE III. The found spacing of the lattice planes, Mueller indices and intensities for Nd:YAG together with comparative literature data[38]

2θ (CuKα)	$2\theta_{lit.}$ (CuKα)	$d_{lit.}$/nm	d/nm	(hkl)	I/I_{max}	$(I/I_{max})_{lit.}$
18.205	17.941	0.494	0.493	211	20.75	40
21.030	20.736	0.428	0.426	220	11.48	10
27.890	27.506	0.324	0.323	321	30.86	20
29.835	29.454	0.303	0.302	400	20.25	30
33.430	33.064	0.2707	0.27	420	100	100
36.730	36.327	0.2471	0.246	422	22.83	30
38.290	37.866	0.2374	0.2349	431	9.68	10
41.225	40.798	0.221	0.2188	521	38.72	25
42.685	42.194	0.214	0.212	440	4.46	5
46.660	46.183	0.1964	0.1945	611	57.93	25
51.690	51.129	0.1785	0.1767	631	4.00	5
52.885	52.292	0.1748	0.173	444	32.11	20
55.200	54.616	0.1679	0.1666	640	36.67	35
56.340	55.732	0.1648	0.163	633	13.44	10
57.450	56.858	0.1618	0.1603	642	46.69	30
57.620			0.1598		21.78	

Reflection spectra recorded in far infrared region can give useful information about the quality of the obtained Nd:YAG single crystals. The positions of the phonon modes can show many important properties of any materials. For this reason, FTIR spectra of Nd:YAG single crystals at various temperatures were recorded. These results will be published in a subsequent paper related to the optical properties of the obtained Nd:YAG single crystals.

CONCLUSION

The conditions for growing Nd:YAG single crystals were calculated by using a combination of Reynolds and Grashof numbers. From the hydrodynamics of the melt, the critical crystal diameter D_c was 1.5 cm and the critical rate of rotation changed from $\omega_c = 38$ rpm after necking to $\omega_c = 13$ rpm at the end of the crystal. The value of the rate of crystal growth was experimentally found to be 0.8–1.0 mm/h. Applying a cone angle

of ~30º for the growth of Nd:YAG single crystals, single crystals without a core were obtained.

Concentrated H_3PO_4 was shown to be suitable for both polishing and etching.

И З В О Д

РАСТ МОНОКРИСТАЛА Nd:YAG-a

АЛЕКСАНДАР ГОЛУБОВИЋ[1], СЛОБОДАНКА НИКОЛИЋ[1], РАДОШ ГАЈИЋ[1], СТЕВАН ЂУРИЋ[2] и АНДРЕЈА ВАЛЧИЋ[3]

[1]Институт за физику, Прегревица 118, п. пр. 57, 11001 Београд, [2]Рударско-геолошки факултет, Ђушина 7, п. пр. 162, 11000 Београд и [3]Технолошко-металуршки факултет, Карнегијева 4, 11000 Београд

Монокристали $Y_3Al_5O_{12}$ допирани са 0,8 % теж. Nd (Nd:YAG) расли су у аргону техником раста кристала по Чохралском. Услови раста монокристала Nd:YAG су израчунати коришћењем комбинације Рејнолдсовог и Грасхофовог броја. Вредности критичног пречника и критичне брзине ротације су одређене помоћу једначина динамике флуида. Пречник кистала D_c = 1,5 cm је држан константним за време процеса раста кристала, док се вредност критичне брзине ротације мењала од ω_c = 38 o/min после ширења и постизања жељеног пречника ("обарања круне") до ω_c = 13 o/min при крају кристала. Брзина извлачења кристала је одређена експериментално и кретала се од 0,8–1,0 mm/h. Сагласно нашим ранијим експериментима, као средство за хемијско полирање је потврђена конц. H_3PO_4 на 603 K при излагању од 20 минута. Конц. H_3PO_4 на 493 K при излагању од 1 сата се показала као погодно средство за нагризање. Одређен је параметар решетке a = 1,201 (1) nm помоћу рендгенске дифракционе анализе праха. Добијени резултати су дискутовани и упоређени са литературним подацима.

(Примљено 17. октобра, ревидирано 17. децембра 2001)

REFERENCES

1. T. Fukuda, K. Shimamura, V. V. Kochurikhin, V. I. Chani, B. M. Epelbaum, S. L. Buldochi, H. Takeda, A. Yoshikava, *J. Mat. Science: Mat. Electron.* **10** (1999) 571
2. D. Jun, D. Peizhen, X. Jun, *J. Crystal Growth* **203** (1999) 163
3. S. E. Kapphan, *J. Lumin.* **83–84** (1999) 411
4. H. A. Wigdor, J. T. Walsh, J. D. B. Featherstone, S. R. Visuri, D. Fried, J. L. Waldvogel, *Laser Surg. Med.* **16** (1995) 103
5. R. R. Monchamp, *J. Crystal Growth* **11** (1971) 310
6. R. F. Belt, R. C. Puttbach, D. A. Lepore, *J. Crystal Growth* **13–14** (1972) 268
7. C. Belouet, *J. Crystal Growth* **15** (1972) 188
8. V. J. Fratello, C. D. Brandle, *J. Crystal Growth* **128** (1993) 1006
9. Y. M. Yu, V. I. Chani, K. Shimamura, T. Fukuda, *J. Crystal Growth* **171** (1997) 463
10. Y. M. Yu, V. I. Chani, K. Shimamura, K. T. Inaba, T. Fukuda, *J. Crystal Growth* **177** (1997) 74
11. V. I. Chani, A. Yoshikawa, Y. Kuwano, K. Hasegawa, T. Fukuda, *J. Crystal Growth* **204** (1999) 155
12. R. S. Feigelson, *J. Crystal Growth* **79** (1986) 669
13. R. S. Feigelson, *Mater. Sci. Eng. B* **1** (1988) 67
14. R. S. Feigelson, *Tunable Solid State Lasers I*, P. Hammerling, A. B. Budgor, A. Pinto, Eds., Springer Verlag, Berlin-Heidelberg-New York-Tokyo, 1985, pp. 129–142
15. Q. Xiao, J. J. Derby, *J. Crystal Growth* **139** (1994) 147
16. K. Kitamura, S. Kimura, Y. Miyazawa, Y. Mori, O. Kamada, *J. Crystal Growth* **62** (1983) 351

17. S. E. Stokowski, M. H. Randles, R. C. Morris, *IEEE J. Quantum Electron* QE-**24** (1988) 934
18. A. Golubović, S. Nikolić, R. Gajić, S. Đurić, A. Valčić, *J. Serb. Chem. Soc.* **64** (1999) 553
19. A. Golubović, S. Nikolić, R. Gajić, S. Đurić, A. Valčić, *Hem. ind.* **53** (1999) 227
20. A. Valčić, R. Roknić, S. Nikolić, *Proc. XXII Symp. ETAN in Marines*, Zadar, Croatia, 1980, p. 354 (in Serbian)
21. A. Valčić, R. Roknić, S. Nikolić, *IRTC S*, Portorož, Slovenija, Elsevier Publ, 1981, p. 505
22. A. Valčić, R. Roknić, S. Nikolić, *Proc. 23. Chem. Symp. of SR Serbia*, Belgrade, Yugoslavia, 1987, p. 627 (in Serbian)
23. A. Golubović, R. Gajić, S. Nikolić, S. Đurić, A. Valčić, *J. Serb. Chem. Soc.* **65** (2000) 391
24. M. T. Santos, C. Marin, E. Diequez, *J. Crystal Growth* **160** (1996) 283
25. J. P. Fontaine, G. P. Extremet, V. Chevrier, J. C. Launay, *J. Crystal Growth* **139** (1994) 67
26. K. Takagi, T. Fukazawa, M. Ishii, *J. Crystal Growth* **32** (1972) 89
27. J. R. Carruthers, *J. Crystal Growth* **36** (1976) 212
28. Q. Xiao, J. J. Derby, *J. Crystal Growth* **128** (1993) 188
29. D. C. Brown, *IEEE J. Quantum Electron.* **34** (1998) 2393
30. V. J. Fratello, C. D. Brandle, *J. Crystal Growth* **128** (1993) 1006
31. M. T. Santos, J. C. Rojo, L. Arizmedni, E. Dieguez, *J. Crystal Growth* **142** (1994) 103
32. C. D. Brandle, *J. Crystal Growth* **57** (1982) 65
33. M. Berkowski, K. Iliev, V. Nikolov, P. Peshev, W. Piekarczyk, *J. Crystal Growth* **83** (1987) 507
34. V. Nikolov, K. Iliev, P. Peshev, *J. Crystal Growth* **89** (1988) 313
35. V. Nikolov, K. Iliev, P. Peshev, *J. Crystal Growth* **89** (1988) 324
36. B. Cockayne, *J. Crystal Growth* **3/4** (1968) 60
37. T. Xu, Z. Wu, W. Peng, Q. Zhen, Z. Xiao, J. Zhou, S. Zhang, S. Xie, C. Huang, Q. Zhou, *Proc. 10th Int. Conf. on Crystal Growth*, San Diego, California, USA, 1992, p. 10
38. JCPDS 38-0222.